Exchange of ATP for ADP on High-Force Cross-Bridges of Skinned Rabbit Muscle Fibers

Chun Y. Seow and Lincoln E. Ford
Krannert Institute of Cardiology, Indiana University, Indianapolis, Indiana 46202 USA

ABSTRACT The contractile properties of rabbit skinned muscle fibers were studied at 1–2°C in different concentrations of MgATP and MgADP. Double-reciprocal plots of maximum velocity against MgATP concentration at different MgADP concentrations all extrapolated to the same value. This finding suggests that MgATP and MgADP compete for the same site on the cross-bridge, and that the exchange of MgATP for MgADP occurs without a detectable step intervening. The K_m for ATP was 0.32 mM. The K_i for MgADP was 0.33 mM. Control experiments suggested that the tortuosity of diffusion paths within the fibers reduced the radial diffusion coefficients for reactants about sixfold. Increasing MgADP from 0.18 to 2 mM at 5 mM ATP or lowering MgATP from 10 to 2 mM at 0.18 mM MgADP, respectively, increased isometric force by 25% and 23%, increased stiffness by 10% and 20%, and decreased maximum velocity by 35% and 31%. Two mechanisms appeared to be responsible. One detained bridges in high-force states, where they recovered from a length step with a slower time course. The other increased the fraction of attached bridges without altering the kinetics of their responses, possibly by an increased activation resulting from cooperative effects of the detained, high-force bridges. The rigor bridge was more effective than the ADP-bound bridge in increasing the number of attached bridges with unaltered kinetics.

INTRODUCTION

Although muscle contraction is powered by ATP hydrolysis, it appears that the immediate source of energy is not hydrolysis of the terminal phosphate bond, but the release of reaction products, notably phosphate, from the cross-bridges (Lymn and Taylor, 1971; Bagshaw et al., 1975; White and Taylor, 1976; Huxley, 1980, p. 93; Taylor, 1992). This observation suggests that energy transduction depends on a highly ordered cross-bridge cycle in which chemical reactions (ATP binding, hydrolysis, product release) alternate with mechanical transitions (cross-bridge attachment, power stroke, detachment). An understanding of the cycle therefore requires an exact knowledge of the number and sequence of transitions in the cross-bridge cycle. The present experiments were undertaken to define the relationship of two chemical reactions, ADP release and ATP binding, to other transitions in the cycle. These reactions were slowed, either by raising the ADP or by lowering the ATP concentrations in skinned fibers. The results support earlier conclusions that ATP exchanges for ADP in high-force states (Cooke and Pate, 1985; Kawai and Halvorson, 1989; Lu et al., 1993), and further suggest that the exchange takes place without a step intervening. In addition, the effects of two separate high-force states, the ADP-bound bridge and the bare, rigor bridge appear to have different effects on contractile performance.

Received for publication 28 February 1997 and in final form 24 March 1997.

Address reprint requests to Dr. Lincoln E. Ford, Krannert Institute of Cardiology, Indiana University, 1111 West 10 St., Indianapolis, IN 46202. Tel.: 317-635-7401, ext. 2965; Fax: 317-267-8730; E-mail: ehomsher@physiology.medsch.ucla.edu.

0006-3495/97/06/2719/17 $2.00

The addition of ADP to the activating solutions precludes the use of an ATP regenerating system. The experimental results were therefore analyzed to determine the effects of radial diffusion on the apparent gradients for ADP and ATP within the fibers. This analysis suggested higher gradients than anticipated and led to further experiments to determine whether other factors increased the gradient. These additional experiments are described under the heading "control experiments" at the end of the Materials and Methods section.

MATERIALS AND METHODS

The methods have been described in detail previously (Seow and Ford, 1992b, 1993). Briefly, adult rabbits of either sex were anesthetized with intramuscular injections of acepromazine (1 mg/kg), xylozine (5 mg/kg), and ketamine (45 mg/kg) and sacrificed by removal of their hearts, which were used in other experiments. Bundles of psoas muscle were skinned by several hours' immersion in ATP relaxing solutions of low divalent cation composition. Fibers were always studied within 1 week of sacrificing the animal, and most were studied within 2–4 days. Some bundles were stored for up to 2 days in relaxing solution at 0°C before use, whereas others were stored for up to 1 week in glycerol solutions at −20°C. Segments of single fibers were held by aluminum foil clips (Ford et al., 1977), so that ~1.5-mm lengths were free between the clips. The clips were used to attach the fibers to a servo apparatus, which controlled one of three parameters: force, sarcomere length, or overall muscle length. The linear servo motor could impose length steps, either sarcomere length or overall muscle length, that were complete within 200–250 μs. Force steps took 1–3 ms to complete. Two types of force transducer were used. For the initial force-velocity experiments photoelectric transducers with resonant frequencies of 5–6 kHz (Chiu et al., 1982) were used. For later experiments on force-velocity and transients, either a piezoelectric transducer adjusted to have a resonant frequency of 10 kHz (Chiu et al., 1978) or an improved version of the photoelectric transducer with a resonant frequency of 15 kHz was used.

Fiber selection

Some of our earlier studies (e.g., Seow and Ford, 1993) were done on fibers from young rabbits weighing ~2 kg. In these earlier studies there was a substantial variation in the maximum velocity of the individual fibers and a spectrum of velocities without a clear division between fast and slow fibers. The present studies were done on older rabbits, weighing ~4 kg, which were sacrificed for other studies. The average maximum velocity in the present study was 25–30% higher than in the previous study when similar conditions were compared, but we noticed that 5–10% of the fibers produced maximum velocities that were half of the higher average or less. No other characteristic, such as diameter, could be used to identify these slower fibers. The results obtained with these slower fibers were excluded. These observations suggest that the higher maximum velocities in the present study were due to our selection of faster fibers and that this selection might have been made possible by a greater differentiation into purer fast and slow fibers in the older rabbits.

Solutions

All experiment solutions contained 56 g/l dextran T-70, sufficient Mg to yield a free ion concentration of 1 mM, sufficient K-propionate to bring the ionic strength to 210 mM, and 10 mM imidazole buffered to pH 7.0. The concentration of dextran T-70 was chosen on the basis of our earlier study (Ford et al., 1991), showing that this concentration reduced maximum velocity to a plateau level that was almost unchanged with further osmotic compression. In studying the effect of pH buffer diffusion, piperazine-*N,N'*-bis(2-ethanesulfonic acid (PIPES), either 10 or 40 mM, was substituted for imidazole. This larger molecule was used because its lower diffusion coefficient was expected to produce a greater pH gradient. Solutions without ADP contained 20 mM creatine phosphate, whereas this constituent was omitted from solutions with ADP. Contracting solutions contained calcium buffered to pCa 4.8 with 5 mM EGTA, relaxing solutions contained 5 mM EGTA, and a rinse solution of 0.1 mM EGTA was used to lower the EGTA concentration immediately before each activation. MgATP and MgADP concentrations were adjusted as described in the Results. The solution composition was calculated using a computer program kindly given to us by Dr. R. E. Godt and using stability constants previously compiled by Godt (1974), Godt and Lindley (1982), Godt and Maughan (1988), Godt and Nosek (1989), and Andrews et al. (1991).

When used, creatine kinase obtained from the Sigma Chemical Co. (St. Louis, MO) was added as the dry powder to rinse and activating solutions. A 3-min rinse period was used, both to allow the enzyme to diffuse into the fibers and to wash it out.

Sarcomere length steps

In the transient experiments, families of nine sizes of sarcomere length steps were applied: two stretches and seven releases. The smaller steps were made as fast as the apparatus would allow, 200–250 μs step duration. The steps were slowed to 3–5 ms for the three largest sizes of release to avoid making the muscle go slack.

Fig. 1 shows the signal-averaged length records for three representative sizes of step. The records of overall muscle length (*thin traces*) are superimposed on the sarcomere length record (*thick traces*). The difference between them, which represents the length change in the nonsarcomere, series elastic elements, is plotted as ordinate against force in Fig. 2. Two plots are shown: the open circles (*steeper curve*) represent the force and length differences at the end of the length step, when the force change was most extreme; the closed circles represent measurements at the end of the recording period. As illustrated, the instantaneous series elastic compliance is about 4 times stiffer than the long-term compliance, as expected from damping of damaged tissue at the ends of the preparation.

For the tension transient experiments described here, the ends of the skinned fibers were fixed with glutaraldehyde before they were clipped (Chase and Kushmerick, 1988). The series elastic element force-extension relations are plotted for these fibers in Fig. 2 *B*, and the data obtained with a similar group of fibers that had not had their ends fixed are shown in Fig. 2 *A*. These plots show that the slopes of both the instantaneous and long-term force-extension plots were reduced twofold by the fixation procedure.

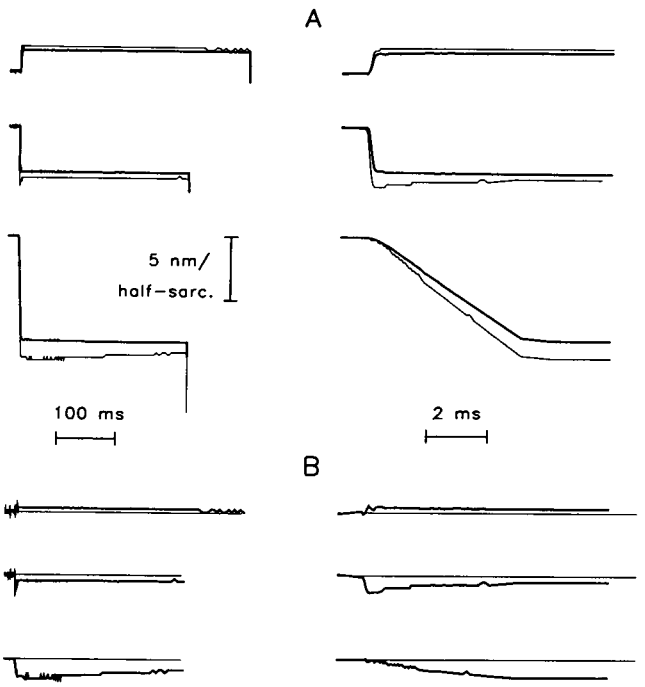

FIGURE 1 (*A*) Overall segment length (*thin trace*), and sarcomere length (*thick trace*) records for three sizes of step used in tension transient experiments. The larger release was slowed to avoid making the muscles go slack. Stretches were recorded for a longer period than releases. Segment length was divided by the number of half-sarcomeres in the segment to display the records in comparable dimensions. (*B*) Difference records (segment length minus sarcomere length) representing the length change of elements in series with the sarcomeres. The left-hand panels show the records from the isometric period until shortly before the end of the recording period, when a large shortening step was applied to zero the transducer by making the fibers go slack, and carry the length records off scale. Records on the right are shown at a speed 50 times greater to resolve the events associated with the step. These are signal-averaged records for 23 fibers activated in 10 mM ATP. The ends of the fibers have been fixed with glutaraldehyde.

The records in Fig. 1 were taken from the family of steps used to define the control tension transient responses in the ATP experiments and are representative of the speed and quality of the steps in all experiments described here.

Protocols

Chemical conditions were always studied in pairs, and the results obtained under one condition (the test) were initially expressed as a fraction of the other (the reference). Where appropriate, the absolute values were calculated from the average values of the reference. Length and force steps were studied in groups of nine during a single activation, using the Brenner (1983) protocol of shortening and restretch to maintain sarcomere homogeneity during continuous activation. Fibers were relaxed between each group of nine steps. For force-velocity experiments, reference conditions always bracketed the test conditions, as previously described (Seow and Ford, 1992b). The bracketing procedure was not used for the tension transient studies. Instead, fibers were made to undergo a series of contractions alternating test and reference conditions. The same size of step

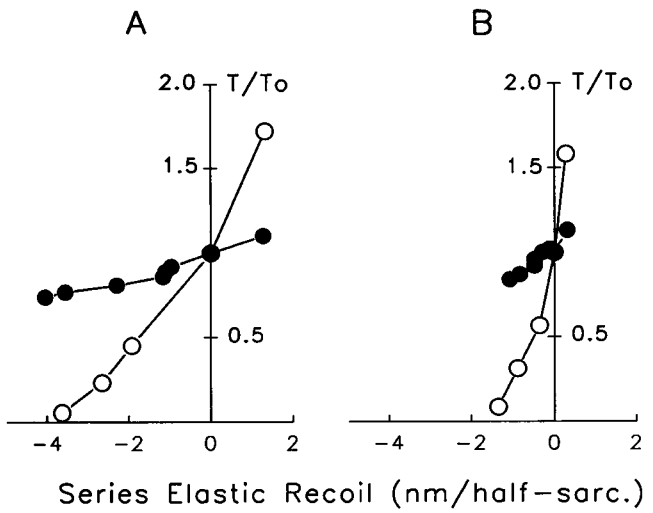

FIGURE 2 Force-extension curves of the series elastic elements (measured as the difference between sarcomere length change and overall muscle length change) of (*A*) fibers from earlier study without fixed ends, and (*B*) same fibers as in Fig. 1 with fixed ends. Open circles show the length difference at the time of the maximum force deviation (i.e., the time of T_1). Closed circles show the difference at the end of the isometric recording period, immediately before the large shortening step was applied. Data values are single measurements of the signal-averaged records.

obtained in two paired contractions that met the selection criteria were then included for analysis.

Criteria for data inclusion

As previously described (Seow and Ford, 1991, 1992b), there was substantial scatter of the velocities at isotonic loads below ~0.01 mN, equivalent to ~2% of isometric force in reference contractions. Force-velocity data were therefore excluded when the force was less than 0.01 mN. No force-velocity points were excluded for any other reason.

There were several criteria for acceptance of data in the tension transient experiments. The main requirement for inclusion was that the sarcomere length signal meet certain specifications. The sensor was calibrated each time a fiber was activated. Before the sarcomere length steps were imposed, the fiber was made to undergo isotonic shortening at ~20% of isometric load for 150 ms. The ratio of the sarcomere length change to the overall muscle length change (the *S/L* ratio) was measured over the last half of this shortening period, when the damped series elastic element changes had ended (Seow and Ford, 1992b). The data were not included unless the *S/L* ratios for two sequential reference and test contractions varied by less than 2%. The values of sarcomere length change given in the results were obtained by dividing the sarcomere length signal by the *S/L* ratio.

After these inclusion criteria were met for a pair of activations including nine steps each, the individual pairs of steps were subjected to additional examination. The additional criteria for inclusion of the individual steps were step speed and freedom from noise. These criteria were more subjective. Pairs of steps from an otherwise satisfactory activation were rejected if either of the steps appeared to be slower than expected or if it contained noise or large perturbations. The major source of noise was spontaneous high-frequency oscillations that sometimes occurred when the system was in sarcomere length control. If either member of a pair of records displayed such oscillations, or other significant perturbations, both were rejected. Because more than one pair of satisfactory activations was usually obtained from each fiber, at least one pair of steps of each size was included from each fiber.

The entire data set for the transient experiments was composed of nine pairs of steps in each of 147 pairs of activations in 48 fibers, for a total of 1323 pairs of steps. Of these, 40 pairs (3%) were excluded for the reasons given above.

Signal averaging of tension transient records

Once pairs of steps were accepted, the records were included for signal averaging into the final result. When more than one satisfactory pair of records for a given step size was obtained from a single fiber, the records from the multiple pairs were averaged to obtain a single pair of records that was included in the final averages. Measurements were made on the averaged records, and the main results are direct comparisons of the averaged records. The principal benefit of this signal averaging was to lower the noise in the records without otherwise distorting the responses.

Data analysis

Force-velocity experiments

The nine force-velocity data points from each of several activations done under the same conditions were pooled and fitted with the Hill (1938) hyperbola,

$$(T - \alpha) \cdot (V - \beta) = -(T_o - \alpha) \cdot \beta \qquad (1)$$

where T is the isotonic force, made dimensionless by dividing by the isometric force measured immediately before the step, V is velocity in units of $\mu m \cdot s^{-1} \cdot$ half-sarcomere^{-1}, and α and β are the force and velocity asymptotes, respectively. The symbols differ from Hill's mainly because two isometric forces are distinguished; one is the zero-velocity intercept of the curve, called T_o, and the other is the isometric tension immediately before the steps, called T_{pre} and expressed in kPa. All experiments were done at a sarcomere length of 2.5 μm (1.25 μm/half-sarcomere), so that a velocity of 1.0 $\mu m \cdot s^{-1} \cdot$ half-sarcomere^{-1} is equivalent to 0.8 muscle lengths/s. The methods of making and analyzing the measurements were identical to those described previously (Ford et al., 1991; Seow and Ford, 1992b, 1993).

For most analytical purposes, the effects of interventions were defined in terms of the relative changes in the physiological parameters, i.e., as the difference in parameters (test minus reference) divided by the reference value.

Tension transient experiments

In tension transient experiments the analysis consisted mainly of direct comparisons of the signal-averaged records. This comparison was facilitated by scaling and subtracting the reference from the test records and examining the difference records. In addition, stiffness was measured as the extreme tension change observed during the step divided by the sarcomere length change $(T_1 - T_{pre})/\Delta S$. The stiffness changes were measured by dividing the test value by the paired reference value for each step size, and then averaging these ratios for all fast steps except the largest fast release. The largest fast release was not included because some of these steps brought tension sufficiently close to zero to make the measurement unreliable.

ATP regenerating system

An ATP-regenerating system consisting of 20 mM creatine phosphate and creatine kinase was used, except when ADP was added to the activating solution. In some experiments, as in our previous studies (e.g., Seow and Ford, 1991, 1992b, 1993), no exogenous creatine kinase was added, and we relied instead on the endogenous kinase in fresh fibers. In other experiments creatine kinase was added as a dry powder to the rinse and activating solutions. This addition raised the pH of these solutions by ~0.01 unit per 50 units/ml of enzyme. For the higher concentrations of enzyme (200 and 500 units/ml) the pH was readjusted. For the lower concentration (50

units/ml) it was not. In all cases, the values of isometric force and velocity were corrected for the small residual differences in pH, 0.003–0.02 units, using the values of 0.5% change in velocity and 0.3% change in force per 0.01 unit of pH (Seow and Ford, 1993).

In studies comparing the presence and absence of creatine kinase, the fibers were soaked in a rinse solution for 3 min before activation to allow the enzyme to diffuse into or out of the fiber. In general, changes in exogenous enzyme were avoided, and the only direct comparison made was between the presence and absence of the kinase at 5 mM ATP. The reference for all solutions with no added kinase was 5 mM ATP, 0 added ADP. The reference for different concentrations of ATP in the presence of kinase was 5 mM ATP. The data obtained in the presence of kinase were then related to that obtained in the absence of kinase by multiplying the relative values (test/reference) by the ratio of the reference values (± kinase).

Control experiments

The finite diffusion distances in skinned fibers create radial gradients for all reactants. Whereas the gradients for ATP and ADP can be minimized with an ATP regenerating system, this regenerating system cannot be used when the effects of elevated ADP concentrations are being studied. Separate control experiments were therefore required to assess the effect of diffusion gradients for reactants on the contractile properties of the preparation. These experiments consisted of measuring changes in isometric force, and maximum shortening velocity produced by an intervention.

ATP regenerating system

This system consisted of 20 mM creatine phosphate plus added creatine kinase. A study of the effect of varying levels of creatine kinase on maximum velocity and force (Fig. 3) suggested that the maximum effects on velocity were achieved with concentrations of 50–100 units/ml. The changes in isometric force were expected to be the opposite of those in maximum velocity, but for unexplained reasons this was not seen at a concentration of 100 units/ml. For this reason, only the results obtained at 200 and 500 units/ml kinase were used. The effect of enzyme concentration on maximum velocity was further evaluated at 2 and 10 mM ATP. The results obtained in 200 and 500 units/ml were identical, and for this reason the two sets of data were pooled in the results described below.

Adequacy of pH buffering

Actomyosin ATPase releases monobasic phosphate, which would contribute ~0.6 mol of hydrogen ion per mole of phosphate at neutral pH. This effect should be reversed, at least partially, by the ATP regenerating system, but in the absence of this regeneration or adequate pH buffering, the released protons would be expected to lower pH. Because the hydrogen ion is carried by a buffer, the pH gradient was assessed from the effect of increasing the buffer from 10 mM to 40 mM. PIPES rather than the usual imidazole was studied because its larger size was expected to create a larger diffusion gradient. The comparison was made in the absence of both creatine kinase and creatine phosphate. As shown in Fig. 3, the velocity obtained was not significantly increased in the higher buffer concentration, suggesting that a pH gradient did not contribute to the velocity differences seen.

Stirred boundary

The effect of added creatine kinase on the intrafiber ADP concentration could be caused in part by the enzymes maintaining a lower ADP concentration at the fiber boundary. A similar effect can be achieved by stirring. To test whether there was a substantial concentration of MgADP at the fiber surface, we compared the effects of stirring with no stirring under conditions expected to produce a large radial gradient. These conditions

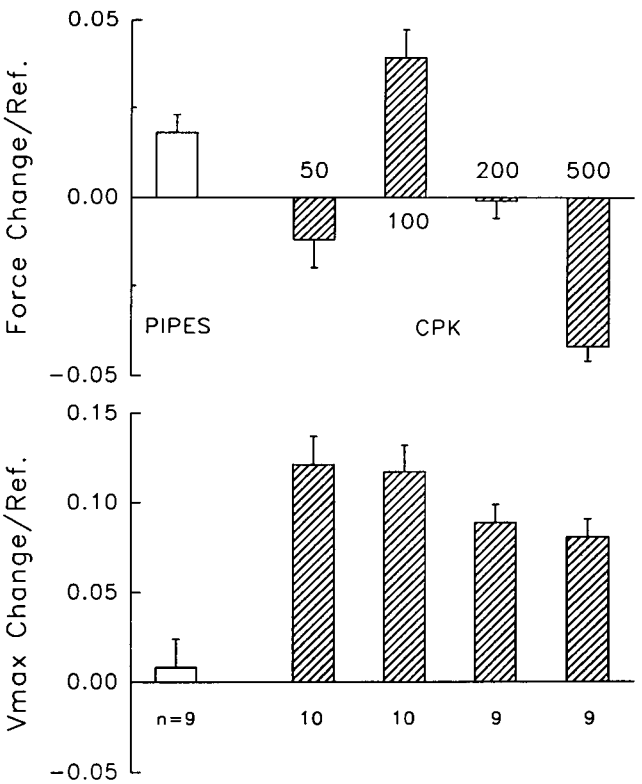

FIGURE 3 Control observations in the presence of 5 mM MgATP, no ADP. (*Top*) Relative force change. (*Bottom*) Relative change in maximum velocity. PIPES: Changes seen when PIPES buffer was increased from 10 to 40 mM. CPK: Changes seen when creatine kinase was added in the concentrations (in units/ml) indicated by the numbers near the force bars. Numbers below the velocity bars indicate the numbers of fibers. Error bars indicate SE.

were 2 mM MgATP in the absence of added ADP, creatine kinase, or creatine phosphate. The stirrer consisted of a solenoid with a plunger that compressed a length of flexible tubing in the line carrying activating solution to the muscle chamber. It was operated at 2 Hz and was adjusted to cause a 2-mm to-and-fro motion of the solution in the muscle trough. This motion was slightly longer than the usual fiber length of 1.5 mm. The results in Fig. 4 show that this stirring produced insignificant differences in developed force and maximum velocity, suggesting that an unstirred boundary had little effect on the intrafiber reactant concentrations. This conclusion would be surprising were it not for the consideration that the Brenner (1983) protocol of releasing and restretching the fibers every 2.5 s is also expected to produce stirring.

Inhibition of sarcoplasmic reticulum and mitochondrial ATPases

Any activity of the sarcoplasmic reticulum or mitochondrial ATPases would contribute to the radial gradient for MgADP and MgATP within the fiber. To test for such a contribution, we compared separately the effects of 5 μM cyclopiazonic acid and 2 mM NaN_3, which are known to inhibit, respectively, the sarcoplasmic reticular and the mitochondrial ATPases (Kurebayashi and Ogawa, 1991). For both interventions the end points measured were isometric force and maximum velocity, and both were measured in the presence of 2 mM MgATP in the absence of both ADP and ATP regenerating systems. Under these conditions, the addition of the full regenerating system would cause maximum velocity to increase by 33%. The NaN_3 caused velocity to increase by an insignificant 6% ($p > 0.05$) and isometric force to increase as well, which was the opposite of the

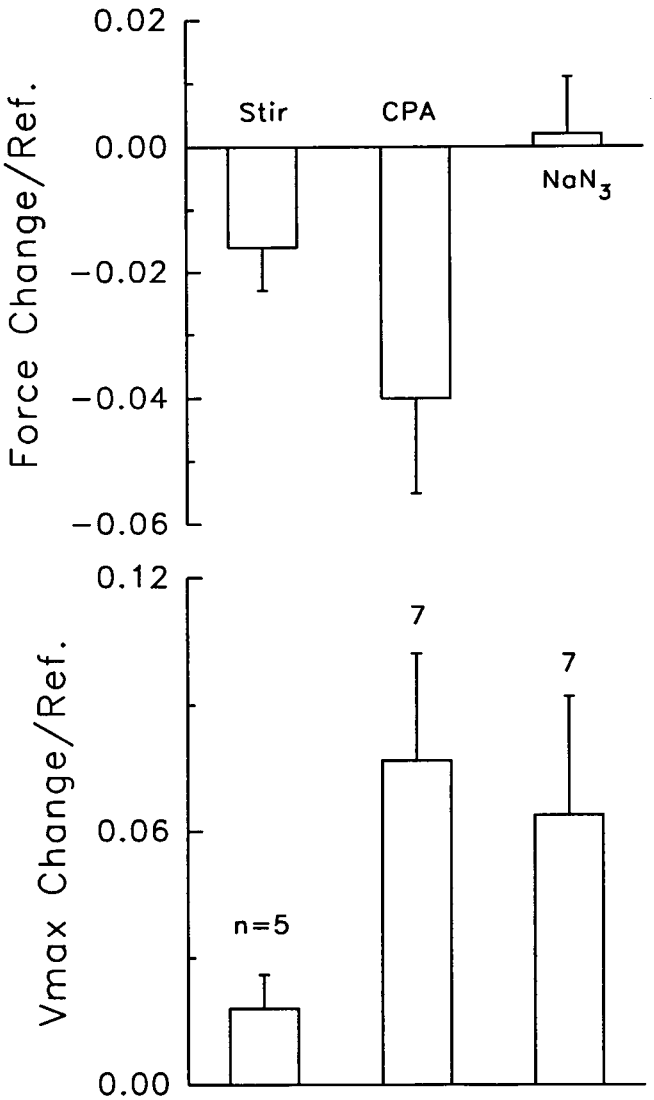

FIGURE 4 Control observations in the presence of 2 mM MgATP, no MgADP, and no creatine kinase. Stir: Changes seen when the solutions were stirred. CPA: 5 μM cyclopiazonic acid. NaN_3: changes seen in the presence of 2 mM sodium azide.

expectation for a decrease in ADP (Fig. 4). The cyclopiazonic acid caused velocity to increase significantly by 7% ($p < 0.05$) and isometric force to decrease, as expected for a decrease in ADP (Fig. 4). These results suggest that 20–30% of the large MgADP gradient may have been due to other ATPases within the fiber, but that most of the gradient was due to other factors.

RESULTS

Many of the experiments were done in the absence of added creatine kinase, relying on the endogenous kinase and 20 mM added creatine phosphate to regenerate ATP. As described below, these conditions resulted in an average MgADP concentration of 0.18 mM within the fibers. Under these conditions, lowering ATP from 10 to 2 mM and raising MgADP from 0 to 2 mM in the presence of 5 mM ATP had qualitatively similar results. Lowering ATP and raising ADP, respectively, decreased maximum velocity by 31% and 35%, increased isometric force by 23 ± 1.0% and 25 ± 1.2%, and increased stiffness by 20 ± 2.0% and 10 ± 1.7% (mean ± SE, n = 23 and 25, respectively). An important point to be made from these changes is that although the force and stiffness increases caused by the two interventions were similar, the ratios of these changes were very different. The ratio of the force increase to stiffness increase caused by adding ADP was 2.5, whereas that caused by lowering ATP was only 1.15.

The effects on the force-velocity relations and the tension transients are described separately.

Curvature of the force-velocity relations

Although the effects of raising ADP and lowering ATP concentrations on isometric force and maximum velocity were very similar, the two interventions produced somewhat different effects on the curvature of the force-velocity curves. To quantify these differences, the force-velocity relations were studied in paired conditions in the same fibers. These fibers, 25 for the ADP experiment and 23 for the ATP experiment, are the same as the ones used to define the effects of the tension transient described below.

All of the force-velocity curves were moderately curved, with relative force asymptotes, α/T_o, in the Hill (1938) equation ranging from 0.128 to 0.198. Adding 2 mM MgADP increased the value of α/T_o from 0.128 to 0.198 and decreased the velocity asymptote, β, from 1.20 to 1.16. Paired t-tests of the relative changes in the two parameters indicated that the changes in α/T_o were highly significant ($p < 0.001$), and that the changes in β were highly insignificant ($p > 0.9$). As previously described (Seow and Ford, 1993), a constant β suggests that the decrease in velocity can be explained by an increased internal load (L), calculated as

$$L = T_{ot} \cdot [(\alpha/T_o)_t - (\alpha/T_o)_r]/[1 + (\alpha/T_o)_r] \qquad (2)$$

where the subscripts r and t indicate the reference and test values, respectively. To the extent that this is so, the values obtained here suggest that all of the differences in shortening velocity could be explained by an internal load equivalent to 6% of isometric force measured in the presence of ADP.

Lowering MgATP from 10 to 2 mM had somewhat different effects on the force-velocity curves. The value of β decreased significantly ($p < 0.01$) by 19%, from 0.149 to 0.121, whereas α/T_o increased significantly ($p < 0.01$), from 0.143 to 0.167. These changes indicate that only a part of the decreased maximum velocity could be explained by an internal load, and that some additional mechanism was also operative. The internal load calculated from the increase in α/T_o was equivalent to 2% of isometric force measured at the lower ATP concentration, equivalent to one-third of the internal load produced by 2 mM ADP. Therefore, a possible explanation of these results is that

33% of the velocity decrease seen at the lower ATP resulted from a mechanism similar to that seen with increased ADP, whereas the remainder was due to a different mechanism. Support for this possibility was found in the tension transient measurements, described below.

Maximum velocity

This varied directly with MgADP concentration and inversely with MgATP concentrations. Plots of the inverse of maximum velocity against the inverse of MgATP concentration at different levels of MgADP or in the presence of two different ATP regenerating systems are shown in Fig. 5. These plots were very nearly linear for different MgADP or creatine kinase concentrations, and all extrapolated to nearly the same value. As shown, the slopes of the lines increased as the concentration of MgADP was increased, both by reducing the ATP regenerating system and by adding MgADP.

The plots in Fig. 5 *A* are similar to Lineweaver-Burk plots used to estimate the dynamics of reversible enzyme inhibition (White et al., 1959, p. 234–249). These plots relate maximum velocity (V_{max}) to ATP concentration (T), ADP concentration (D), Michaelis constant (K_m), inhibitory constant (K_i), and the inverse of absolute maximum velocity (A) by the equation

$$1/V_{max} = A \cdot (1 + K_m/T + K_m \cdot D/K_i \cdot T) \quad (3)$$

In this formulation K_m is equivalent to the MgATP concentration at which maximum velocity is half the absolute maximum in the absence of ADP, and K_i is the equivalent to the MgADP concentration at which the K_m is twice the value obtained in the absence of ADP. The values of K_m and A were determined from the slope and intercept of the line fitted to the data obtained in the absence of ADP and in the presence of sufficient regenerating system to saturate the velocity response (data set [*diamonds*] fitted by the lowest lines in Fig. 5). These fitted values were 0.32 ± 0.02 (SE) mM for K_m and 1.01 $\mu m \cdot s^{-1} \cdot$ half-sarcomere^{-1} for absolute V_{max} (equivalent to the inverse of 0.87 times the reference value of 0.88 $\mu m \cdot s^{-1} \cdot$ half-sarcomere^{-1}).

The value of K_i could be estimated crudely from the lines fitted to the data in Fig. 5 *A*, but the velocities measured in the absence of an ATP regenerating system are reduced by both increased ADP and decreased ATP concentrations. To estimate the intrafiber concentrations for these reactants, as well as to determine the inhibitory constant, the data for the three highest data sets in Fig. 5 were fitted to a modification of Eq. 3 that accounted for intrafiber ATP hydrolysis. This analysis relates the intrafiber MgADP and MgATP concentrations, D_i and T_i, respectively, to shortening velocity and the bath concentrations, D and T, by

$$D_i = D + d \cdot c \cdot V_{max} \quad (4)$$

$$T_i = T - c \cdot V_{max} \quad (5)$$

This analysis assumes 1) that the rate of ADP production equals the rate of ATP depletion, but that only a fraction of the ADP, equal to d, is in the MgADP form that inhibits shortening; 2) that the rate of ATP hydrolysis is related to the measured maximum velocity by the proportionality constant c; 3) that the intrafiber gradient has the same effect as a mean concentration difference of the same magnitude; and 4) that the diffusion rates for ADP and ATP are the same. Substituting the D_i and T_i in Eqs. 4 and 5 for D and T in Eq. 3 yields

$$1/V_{max} = B/2 + [B^2 - 4 \cdot A \cdot c \cdot (1 - d \cdot (K_m/K_i)/T]^{1/2}/2 \quad (6)$$

where $B = A + c/T + A \cdot K_m/T + A \cdot D \cdot K_m/K_i \cdot T$. The program that calculated the solution concentrations indicated that ~39% of the ADP was bound to Mg under the conditions used here, and so d was assigned the value 0.39. A least-squares method was used to determine K_i and c from the data obtained in the absence of creatine phosphate and varying levels of added MgADP (three upper sets of data in Fig. 5), using the values of A, k_m, and d previously assigned. Fig. 5 *B* plots the curves derived from a nonlinear, least-squares fit of Eq. 6 to the data. The values of K_i and c determined from these fits were 0.33 mM and 1.67 mM · half-sarcomere · s/μm, respectively.

The data obtained in the presence of 20 mM creatine phosphate and no added kinase (Fig. 5, *circles*) could not be fitted with the least-squares method because the amount of ADP removed by the partial regenerating system could not be estimated in advance. A fit was later obtained by another least-squares fit to Eq. 6 (Fig. 5 *B*, *dotted curve*) that determined a negative value of added MgADP using the values of the other five parameters previously assigned.

Estimation of intrafiber concentrations of ATP and ADP

The value of c determined by the fitting procedure implies that the intrafiber MgADP concentration was 0.7 mM higher than the bath concentration at the absolute maximum velocity in the absence of an ATP regenerating system. A graphical method of estimating these concentrations is shown in Fig. 6; the K_m's derived from the initial slopes of the fitted curves at infinite ATP concentration (K_{mi}) are plotted against the added MgADP. The line fitted to the data obtained without the regenerating system (*filled circles*) is extrapolated to negative values of added MgADP to determine the amount of MgADP removed by the regenerating system.

The utility of this graphical method is that it allows an estimation of the MgADP subtracted by partial regenerating systems. An example is shown by the open circles representing the K_m for the data obtained in the presence of the regenerating system. The uppermost of these two points represents the K_m obtained in the presence of creatine phosphate but no added creatine kinase. The interpolation sug-

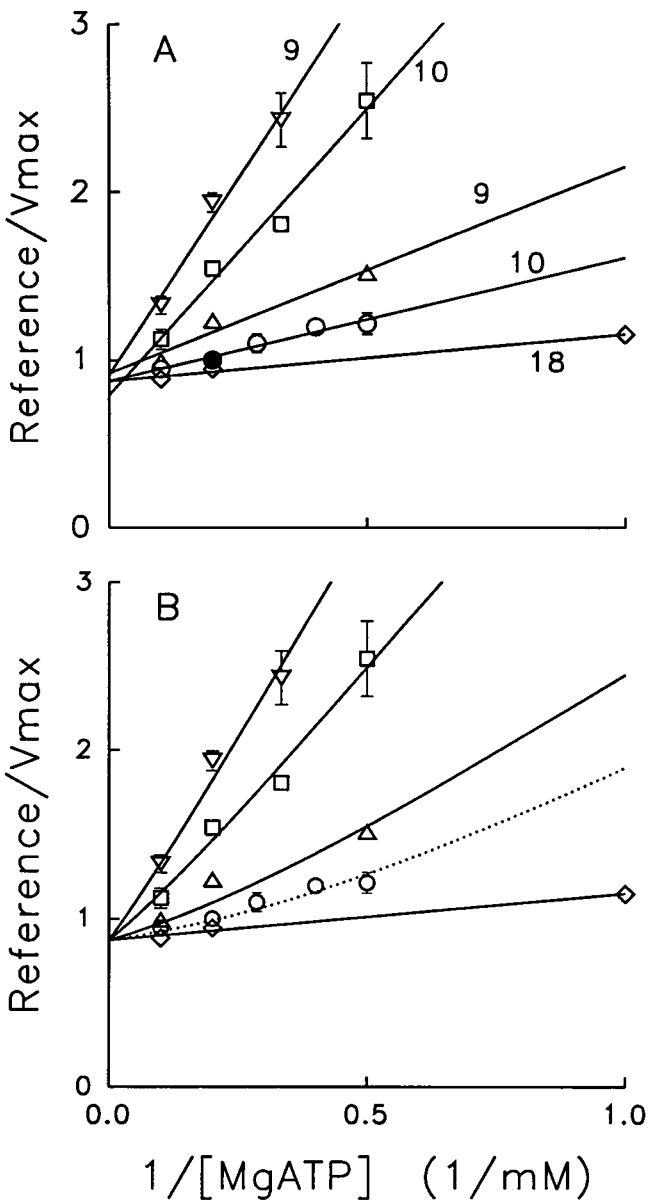

FIGURE 5 Inverse of maximum velocity versus inverse of MgATP concentration. From the bottom up, the data sets are as follows: ◆, full regenerating system containing 20 mM CP, and either 200 or 500 units/ml CK (results averaged for the two concentrations); ○, partial regenerating system containing 20 mM CP; △, no regenerating system, no added ADP; □, 2 mM added MgADP; ▽, 4 mM added MgADP. For data obtained without CK, the reference condition was 5 mM MgATP, 20 mM CP, no added MgADP (●), and the reference velocity was 0.88 $\mu m \cdot s^{-1} \cdot$ half-sarcomere^{-1}. For data obtained with added CK, the reference was 5 mM MgATP. The two data sets were combined by multiplying the velocities obtained with CK by the ratio of the CK reference to non-CK reference. The lowest data set was fitted with a straight line to determine the inverse of absolute maximum velocity, A, and the MgATP concentration at which maximum velocity was half, K_m. (*A*) Four upper data sets fitted with straight lines. (*B*) Three upper data sets fitted with Eq. 6, using a least-squares method to find K_i and c. Second data set from bottom (*dotted line*) fitted by a separate least-squares determination of the reduction of MgADP in the partial regenerating system, using the previously determined values of A, K_m, and K_i. Error bars indicate SE. Data points without error bars had a SE equivalent to less than the size of the symbol. Numbers next to each line indicate the number of fibers studied, which was the same for all points on a line.

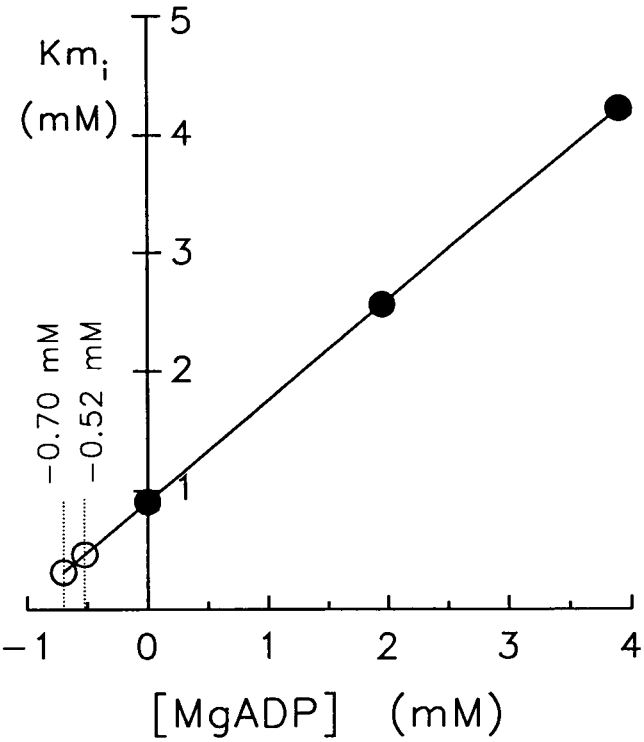

FIGURE 6 Values of K_m for infinitely high MgATP concentrations (K_{mi}), determined from the initial slopes of the curves in Fig. 3 *B*, plotted against added MgADP concentration. Extrapolation to negative values of added [MgADP] (○) to estimate the MgADP removed by the regenerating systems. Lowest value, 20 mM CP, and added CK. Second lowest, 20 mM CP, no added CK. Vertical numbers indicate the estimated value of MgADP removed.

gests that the partial regenerating system removed 0.52 mM MgADP, 0.18 mM less than the full regenerating system. Thus it is estimated that the average intrafiber concentration of ADP in the absence of added creatine kinase was ~0.18 mM.

Tension transients

To learn more about how ADP and ATP interact in the cross-bridge cycle, the effects of these metabolites on the tension transients were studied. The fibers were activated continuously while nine different sizes of sarcomere length step were applied. These progressed from the largest stretch to the largest release. The step sizes were adjusted so that the fourth release would bring force at the end of the step near zero under the reference conditions. This step size was divided by 4 to obtain a length change increment. The two stretches were two and one of these increments, respectively. The first four releases were increased progressively from one to four of these increments. The next three releases were increased by two increments each. The two stretches and four smallest releases were made at the maximum speed, a step duration of 200–250 μs. The three larger releases were slowed to avoid making the muscle go slack when sarcomere length was being servo controlled. The

seventh and eighth step duration was increased to ~3 ms and the ninth to 5 ms. The resulting force transients showed the four characteristic phases described by Huxley and Simmons (1971, 1973).

Effects of added ADP

A selection of force responses to step changes of sarcomere length are shown in Fig. 7 *A*. Pairs of records made in the presence (*thick traces*) and absence (*thin traces*) of 2 mM MgADP are superimposed in Fig. 7 *A*, so that the isometric force levels at the beginning of the record coincide. The 25% greater isometric force achieved in the presence of ADP is shown as a downward displacement of the zero force baseline at the end of the test records. The difference records, reference minus test, for seven step sizes are plotted in Fig. 7 *B*. (The records for the smallest stretch and release have been omitted.) The 10% increase in stiffness is represented by a change in the difference record that develops during the step itself. This difference remained nearly constant during the early, rapid, phase 2 force recovery and then declined slowly as the steady-state isometric differences were reestablished. The flatness of difference records after the step ends indicates that the time course of the early, rapid, phase 2 force recovery was the same under both conditions.

As discussed below, we interpret these results as indicating that MgADP detains some cross-bridges, leaving others to function normally. To estimate the response of the abnormal bridges, the response obtained under reference conditions is scaled, to account for an alteration in the number of normal bridges, and subtracted from the test response. In the present instance, no scaling was required to make the amplitude and time course of phase 2 recovery coincide.

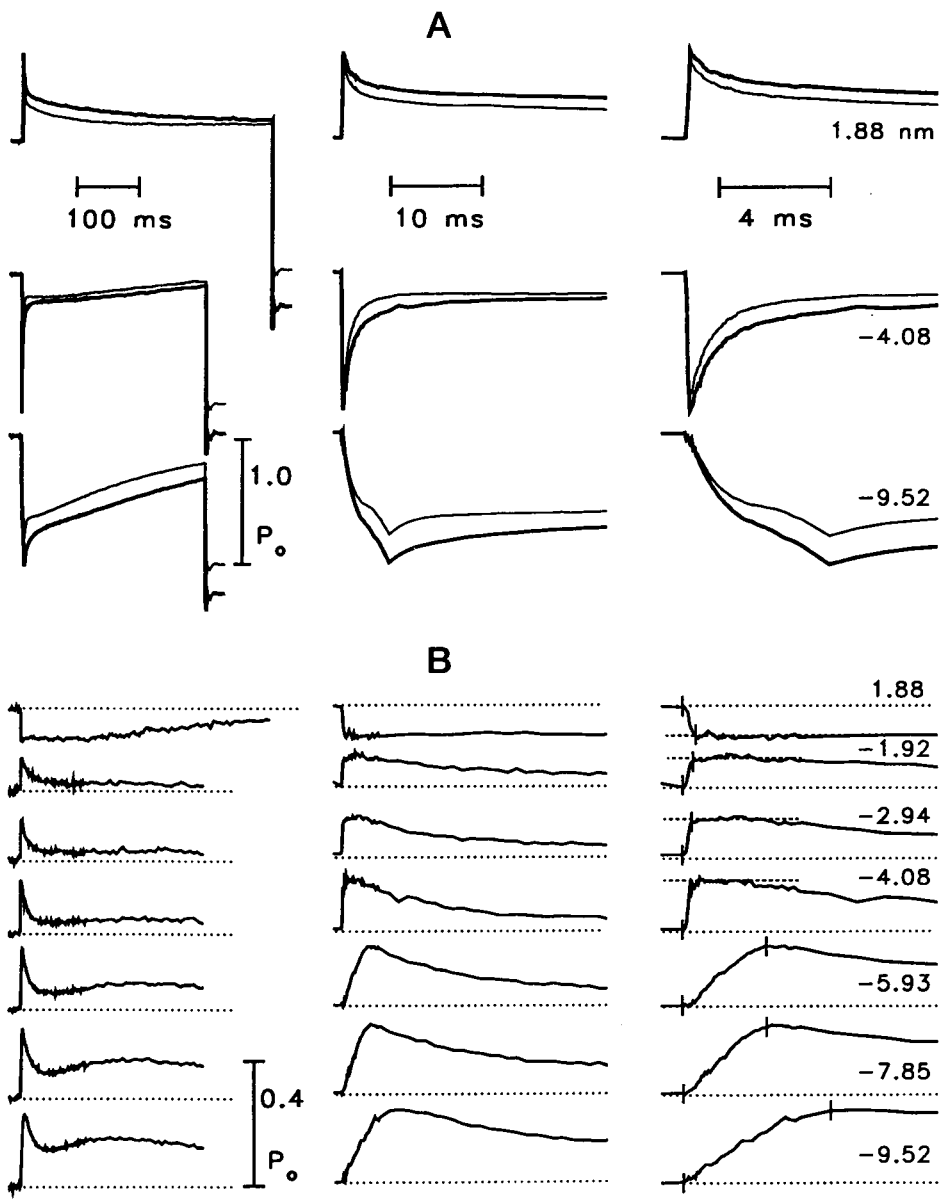

FIGURE 7 (*A*) Signal-averaged, paired force responses to step changes of sarcomere length in the presence (*thick trace*) and absence (*thin trace*) of 2 mM MgADP for 25 fibers. Responses to three selected sizes of step are shown: the largest stretch, a fast release that would bring instantaneous force almost to zero, and the largest, slowed release. Records have been shifted so that their isometric forces coincide. (*B*) Difference records (reference minus test) amplified 2.5 times for seven step sizes. Records for smallest stretch and release have been omitted. Left-hand panels show the entire record. Middle and right-hand panels show the records on faster time bases. Vertical cursors on the fastest difference records indicate the onset of the step and the time of the extreme tension change (T_1). Numbers next to the record indicate the size of step in nm/half-sarcomere. The interrupted horizontal lines on the high-speed records indicate a constant difference. The computer plotting routine slightly exaggerated the amplitude of compressed high-frequency noise in the slow-speed records.

This result suggests that there had been very little change in the number of normally functioning isometric bridges that produced the rapid, phase 2 force recovery.

Effects of varying ATP

Records similar to those of Fig. 7 are shown for 10 mM (*thin traces*) and 2 mM (*thick traces*) MgATP in Fig. 8. As with adding MgADP, lowering the MgATP concentration increased both force and stiffness, but the increased stiffness was substantially larger than that seen with added MgADP, as shown by the greater deviation of the difference traces of Fig. 8 *B*. The 23% increase in force caused by lower MgATP was associated with a 20% stiffness increase. In addition, the force difference that developed during the step declined rapidly during phase 2. This response is very different from that obtained in the presence of MgADP. It seems likely that the responses of the bridges detained by the two interventions would be similar in character, even if they had different rate constants. As a result of this expectation, the reference records were scaled to match the speed of phase 2 force recovery, similar to the match of the difference records obtained in the ADP experiment of Fig. 7. The match was judged by the flatness of the difference record obtained by subtracting the scaled reference record from the test record. The flattest difference records were obtained when the reference records were scaled up by 18% (Fig. 9). Scaling by this factor, therefore, represents an end

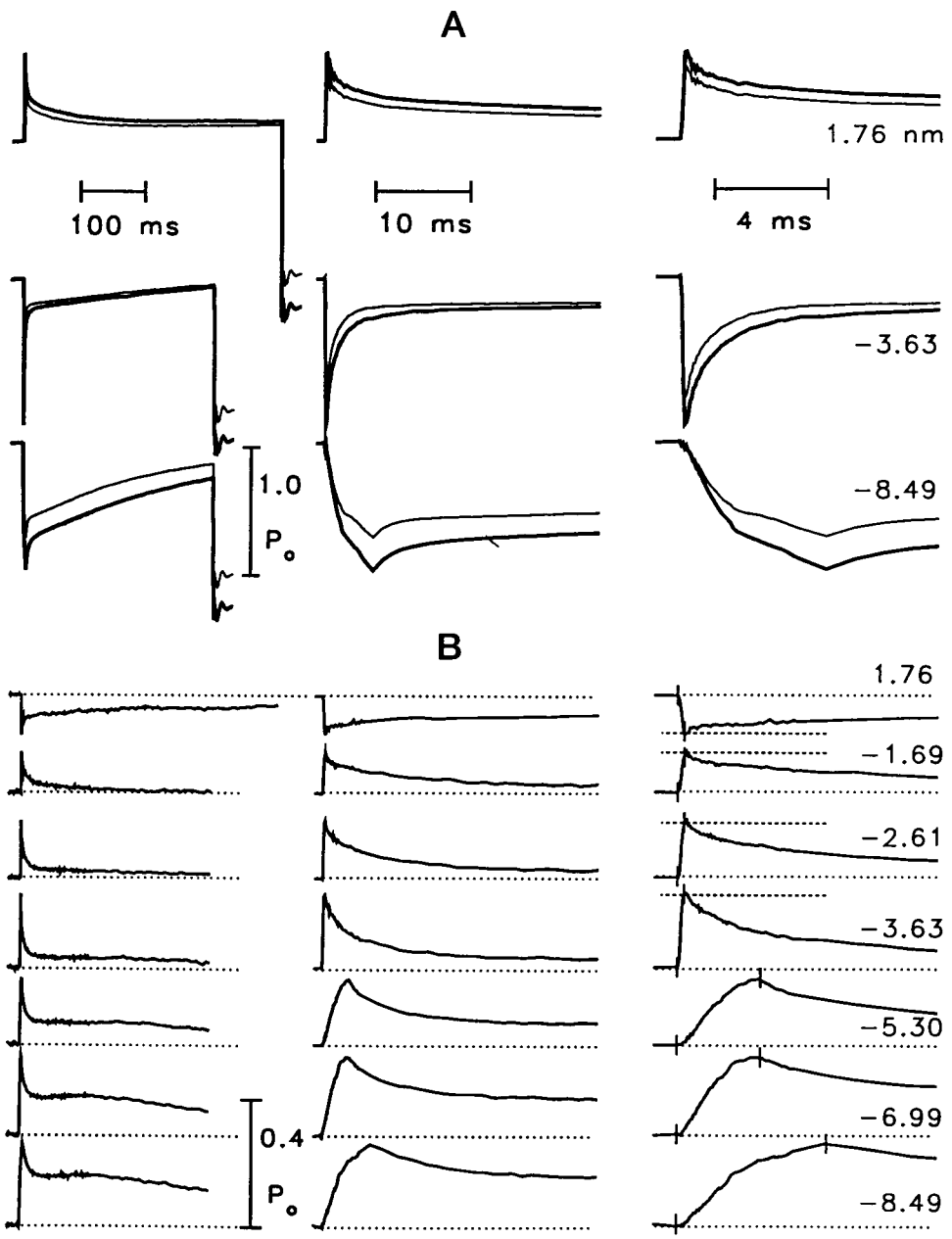

FIGURE 8 Effect of lowering MgATP from 10 mM (reference, *thin traces*) to 2 mM (test, *thick traces*) on the tension transients. Display as in Fig. 7. Signal-averaged records from 23 fibers.

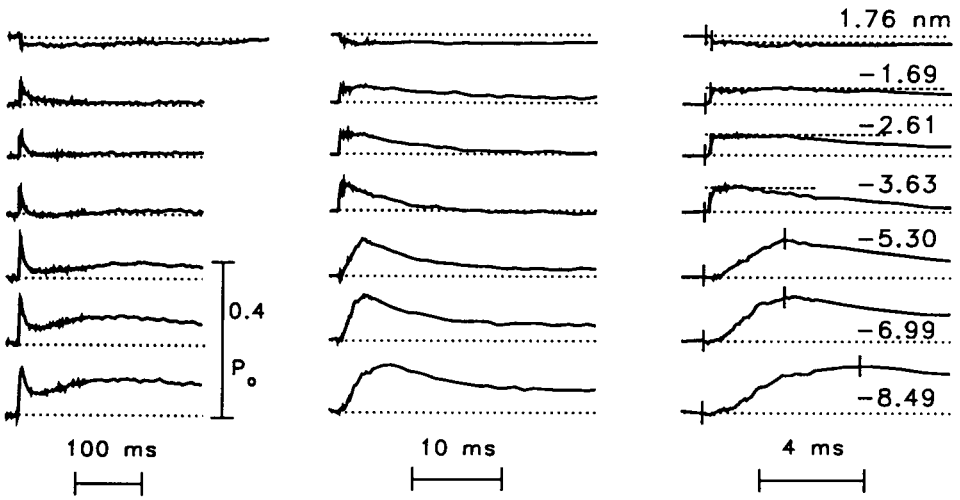

FIGURE 9 Difference records obtained by scaling the reference records to obtain the coincidence of the phase 2 force recovery in the ATP experiment. As indicated, the reference records were scaled by 1.18. The records for the smallest stretch and release have been omitted.

point where the early responses are the same under the two conditions.

Recovery of the difference records

The difference records on Figs. 7 and 9 show that the initial flat part of the record during phase 2 was followed by a decline to a level that was nearly constant for small releases and that reached a nadir for the larger releases. Analysis of the recovery after phase 2 showed that each difference record could be fitted with a single exponential. The time constants for the ATP experiment were about twice those for the ADP experiment, and they varied slightly with step size, being fastest for intermediate sizes of release. The highest rate constants, for intermediate sizes of step, were 0.06/ms and 0.14/ms, respectively, for the ADP and ATP experiments. For both conditions, the values were 33–50% of the highest values for the smallest releases and 50–75% of the highest values for the largest releases.

T_1 and T_2 curves

The extreme tension reached at the end of the step (T_1) and the tension level approached during the partial, rapid, phase 2 force recovery (T_2) are plotted in Fig. 10. As shown, the T_2 levels scaled in almost exact proportion to the isometric force. As discussed below, the fraction of attached bridges in high force states can be estimated from the ratio of the zero-force intercepts of the two curves after correction for cross-bridge movements that occur over the measurement interval. The T_1 curves reached zero at about 4 nm/half-sarcomere, but as described previously (Ford et al., 1977), these curves are rounded slightly by the rapid recovery of force during the larger releases. The intercept of the curve extrapolated from stretches, ~3.5 nm/half-sarcomere, therefore gives a better estimate of the sarcomere compliance, the quantity of interest in these estimates. The T_2 curves extrapolated to zero at ~14 nm/half sarcomere, but this intercept might be increased by detachment of negative-force bridges during phase 2 recovery. As discussed below, our best estimate of the ratio of the intercepts is 4, but it could be less.

DISCUSSION

The main conclusion from this study is that ATP exchanges for ADP on cross-bridges that are attached in a high-force state. The observation that increasing the MgATP concentration overcame the inhibitory effect of MgADP suggests that the two metabolites compete for the same site on the contractile proteins. The observation that the double-reciprocal plots extrapolated to the same maximum velocity (Fig. 5) further suggests that the exchange occurs without a detectable intervening step. If this were not the case, if an additional transition between the release of ADP and the binding of ATP imposed a delay, it would not be possible to overcome completely the inhibitory effect of ADP by increasing the ATP concentration. The decreased velocity caused by both the increased ADP and the decreased ATP suggests that both interventions decreased cross-bridge cycling rates. Finally, the observation that both interventions increased force out of proportion to stiffness indicates a higher average force per attached bridge, and suggests that both interventions detained cross-bridges in high-force states.

This conclusion is not surprising. It is expected that ATP will exchange for ADP; because ATP is hydrolyzed to ADP, the two ligands probably occupy the same binding site, and therefore must exchange. The expectation that the exchange occurs on a high-force state derives from both anatomical and chemical studies. The electron microscope finding of Reedy et al. (1965) that rigor bridges are attached to thin filaments at an angle suggests that they have completed their power stroke and are in a high-force state. The finding of Lymn and Taylor (1971) that rigor bridges are dissociated from actin very rapidly by ATP suggests that the binding of ATP is one of the last transitions that a bridge undergoes before it detaches.

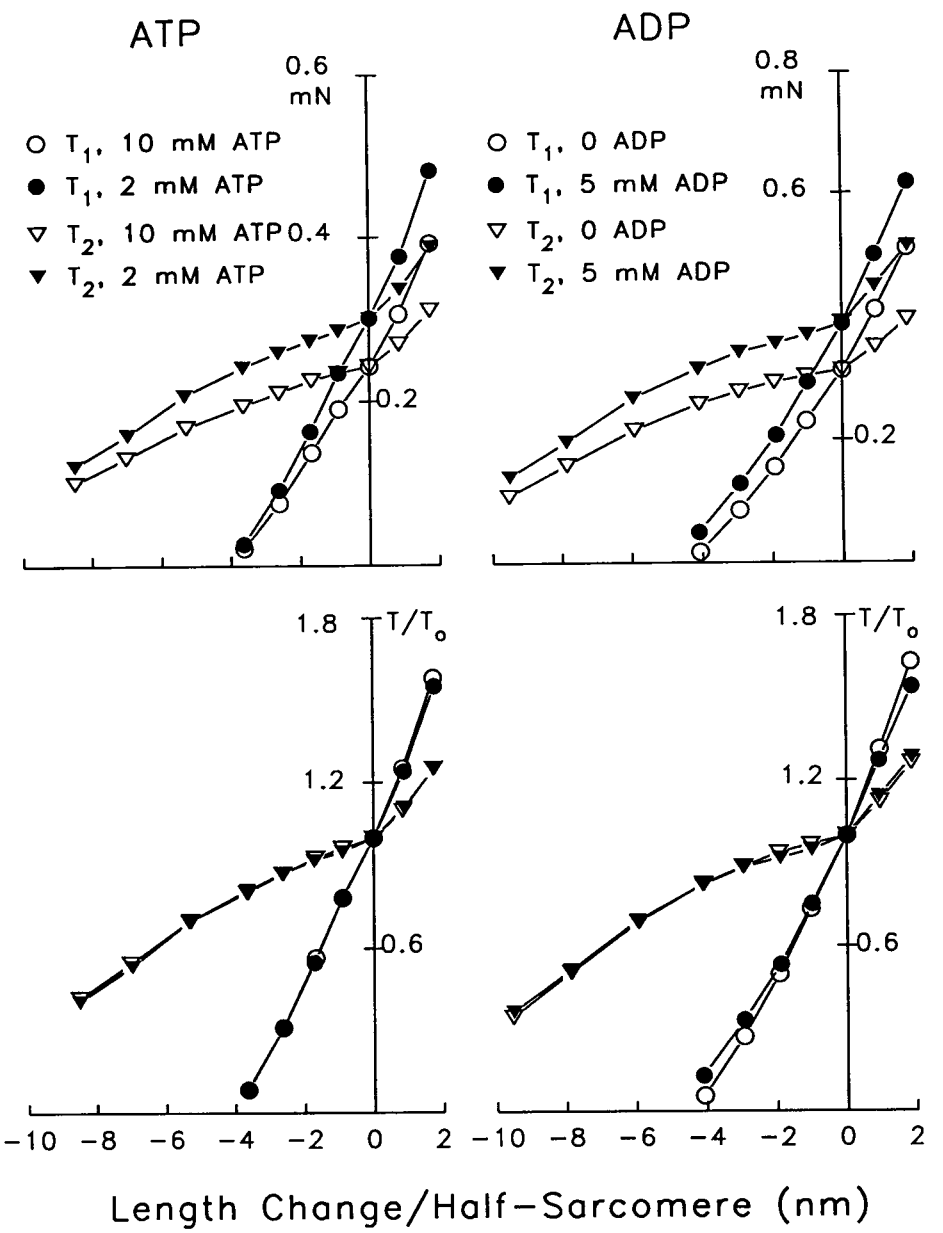

FIGURE 10 Extreme force reached at the end of step (T_1) (○, ●), and force approached during Phase 2 (T_2) (▽, ▼) versus sarcomere length step. Reference conditions (○, ▽) were 5 mM MgATP without added ADP (*left*) and 10 mM MgATP (*right*). Test conditions (●, ▼) were 2 mM MgATP (*left*) and 2 mM MgADP (*right*). Absolute forces are plotted in the upper panels, and forces normalized to the isometric value are plotted in the lower panels.

The main significance of the present findings is that they extend the earlier conclusions regarding the mechanical scheme to show that there are two distinctly different high-force states created by the two interventions, that the two states have different properties, and that the transition between them occurs without a state intervening.

Relationship to earlier work

Isometric force

The force-enhancing effects of increased MgADP and/or lowered MgATP are well known (Abbott and Mannherz, 1970; Cooke and Bialek, 1979; Cooke and Pate, 1985; Hoar et al., 1987; Kawai and Halvorson, 1989; Lu et al., 1993). Furthermore, some of this earlier work has shown that it is the MgADP and not the free ADP that is responsible for the force increase (Ferenczi et al., 1984; Hoar et al., 1987; Lu et al., 1993). Cooke and Pate (1985), Kawai and Halvorson (1989), and Lu et al. (1993) have further demonstrated that MgATP binds to the same cross-bridge site as MgADP. The work of Dantzig et al. (1991) on the effect of ADP on the relaxation from rigor by photogeneration of caged ATP also suggests that ADP and ATP compete for binding to cross-bridges. The present results are in agreement with all of this earlier work and, as mentioned, extend the conclusion to suggest that ATP and ADP exchange without a detectable intermediate step.

Kinetic constants

Ferenczi et al. (1984) found the K_m for the interaction of MgATP with skinned frog fibers at 0–5°C to be 0.47 mM.

Cooke and Pate (1985) found the K_m for rabbit psoas fibers to be ~0.15 mM and the K_i to be 0.2–0.3 mM ADP at 10°C. Our value for K_m is midway between the two prior studies, whereas our value of K_i is near the upper limit found by Cooke and Pate. There are, however, major differences in the three studies that should be recognized. The study of Ferenczi et al. was made in a different species, and the study of Cooke and Pate was made at substantially higher temperature. Perhaps most importantly, the use of high-molecular-weight polymers to compress the fiber lattice in the present study is likely to have such substantial effects that the good agreement with the earlier work is surprising. The original cross-bridge theory (Huxley, 1957) predicts that the well-defined maximum velocity achieved at zero force results from a balance between the bridges that are attached and generating positive force, and the bridges that have moved through their useful range but remain attached to resist further shortening. Goldman (1987) showed that skinned fiber maximum velocity was higher than that of intact fibers, unless the fibers were osmotically compressed. In addition, he used Huxley's (1957) equations to show that this increased velocity was explained quantitatively by the inability of the spent bridges to resist continued shortening. Thus the results obtained in noncompressed skinned fibers and in isolated proteins, where there is no interaction between individual bridges, are likely to give different results from intact muscle fibers and compressed myofibrils. To the extent that maximum velocity in intact or compressed fibers is dependent upon detachment of bridges after the exchange of ATP for ADP, the effects of varying these metabolites will be underestimated in noncompressed fibers and isolated proteins.

Transient responses

Kawai and Halvorson (1989) studied the responses of skinned fibers to sinusoidal oscillations with frequencies up to 250 Hz and concluded that increased ADP or decreased ATP concentrations diminished the speed of their fastest response (Process C, corresponding to late phase 2 of the tension recovery described here). The present results agree with this finding, but also suggest that it is only the slower and/or later components of the response that are affected. Lu et al. (1993) have shown that the photogeneration of ADP in skinned fibers at 15°C causes force to increase with a rate constant approaching the overall cycle time for the cross-bridges. They conclude that the increase in force is due to a decrease in cross-bridge detachment, with redistribution of bridges into high-force states. The present results suggest that at least some of the observed force increase is due to this mechanism, but that an additional mechanism is required, at least under the conditions used here.

Competitive inhibition

The force-velocity data can be interpreted quantitatively in terms of a scheme in which added MgADP competes with MgATP for binding to high-force bridges without ligand. This scheme is shown in Fig. 11 *A*, together with the enzyme reactions for which Michaelis-Menten and Lineweaver-Burk kinetics were derived (Fig. 11 *B*) (White et al., 1959, pp. 234–239). Michaelis-Menten enzyme kinetics describe exactly a reaction sequence in which enzyme binds substrate reversibly and then undergoes an irreversible step that releases the enzyme. To the extent that the detachment of the myosin-ATP cross-bridge is not reversible, this scheme will accurately describe the reaction of ATP with cross-bridges. Lineweaver-Burk plots, such as those in Fig. 5, can be used to show that the inhibition is competitive, as in Fig. 11 *B*. The major difference between the enzyme kinetic scheme and the cross-bridge cycle is that the enzyme-inhibitor complex is in equilibrium, whereas the actomyosin-ADP complex is in a steady state. The finding that the Lineweaver-Burk plots give a good description of the muscle behavior suggests that this difference does not cause a substantial deviation from the scheme shown in Fig. 11 *B*, at least under the conditions studied.

Analysis of the transients

The results are interpreted here in terms of the scheme shown in Fig. 11 *A*. It should be emphasized both that this simplified scheme does not include all transitions known to occur and that the interpretation requires at least one mechanism not accommodated by the scheme, as will be described. Furthermore, the scheme is made as simple as possible, assuming a single power stroke per attachment cycle. In the scheme shown, bridges attach in a low-force state and undergo at least one chemical transition before undergoing a power stroke that moves them to high-force states, where they undergo several more chemical transi-

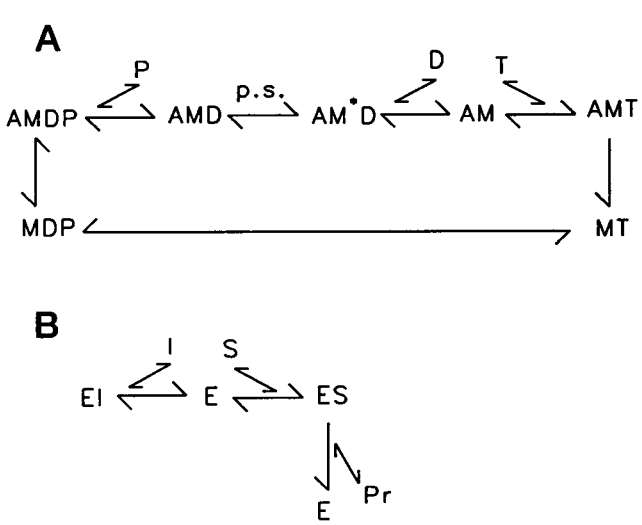

FIGURE 11 Reaction schemes. (*A*) Interaction of ADP (D) and ATP (T) in the actin (A) and myosin (M) cycle including a power stroke (p.s.). (*B*) Michaelis-Menten enzyme (E) interaction with substrate (S), product (Pr), and inhibitor (I), showing the similarity to the cross-bridge cycle.

tions before detaching. It is further assumed that the power stroke stretches a spring somewhere in the bridge between the actin and myosin filaments (Huxley, 1974), so that the energy required to stretch the spring is included in the activation energy for the power stroke (Huxley and Simmons, 1971). The change in activation energy causes the speed of the early, rapid, phase 2 force recovery to be step size dependent. It is also expected that if the chemical transitions are not associated with alterations in spring tension, their rate constants will not vary much with the size of the step.

The method of analysis used here assumes that the overall tension responses are the sum of the stochastic responses of individual bridges. In this analysis, changes in chemical environment are assumed to alter only one or two transitions (or states), leaving the others unchanged. In terms of the scheme of Fig. 11 *A*, an increased ADP concentration slows the cycle by slowing the transition from the AM*D state to the AM (rigor) state. This slowing causes an increase in the fraction of bridges in states that precede this transition, principally the AM*D state. Because this state follows the power stroke, the bridges in this state increase force out of proportion with their number. Similarly, reducing the ATP concentration slows the transition from the AM to the AMT state and increases the fraction of bridges in both the AM and the AM*D state. Again, because these states follow the power stroke, they increase force out of proportion with their number.

Estimating the fraction of bridges in high-force states

The consideration that force is increased by the detention of bridges in the high-force states that follow the power stroke raises the question of how much the detained bridges should increase force. Uncertainties preclude an exact answer, but the ratio of the T_1 and T_2 intercepts suggest that about one-quarter of the attached bridges are in high-force states, so that an additional high-force bridge should increase force by ~4 times the average produced by attached bridges. To understand this estimate, consider that the bridges attach in a zero force state and that sufficient shortening is applied to keep the force at zero after all of the bridges undergo their power stroke. The amount of shortening needed to keep the force at zero would be the average distance the bridges move during the power stroke. This distance is the value of the T_2 intercept, corrected for any cross-bridge detachment during phase 2. By contrast, the intercept of the T_1 curve represents the distance the bridges have moved to achieve the isometric force, averaged over the entire population of attached bridges. Because some bridges have moved the full distance and some have not moved at all, the ratio of the two intercepts reflects the fraction of the bridges that have undergone the power stroke and are in the high-force states. As stated in the Results, this ratio appears to be ~4, but could be smaller.

These relationships are expressed algebraically as follows. If the attached bridges exist in either high- or low-force states that are separated by an axial distance equivalent to the T_2 intercept (I_2), the force in the fiber (T) is given by

$$T = k \cdot (n_1 \cdot x + n_2 \cdot [x + I_2]) \quad (7)$$

where k is the spring constant for the cross-bridge, x is the axial displacement from the isometric, and n_1 and n_2 are the fractions of bridges in low- and high-force states, respectively. Instantaneous filament displacement equivalent to the T_1 intercept (I_1) reduces the force to zero, so that $T = 0$ and $x = I_1$, so that Eq. 7 becomes

$$0 = k \cdot (n_1 \cdot I_1 + n_2 \cdot [I_1 + I_2]) \quad (8)$$

which can be rearranged to

$$n_2/(n_1 + n_2) = I_1/I_2 \quad (9)$$

The uncertainties in the estimate arise because the intercepts are affected by cross-bridge activity between the onset of the steps and the time the measurements are made. The T_1 values are truncated by detachment of bridges during large releases, so that a more accurate estimate is obtained by extrapolation of the T_1 values for stretches (Ford et al., 1977). This value is ~3.5 nm/half-sarcomere. The T_2 values may be affected similarly by cross-bridge detachment during phases 2 and 3. These effects are minimized by measuring T_2 values as the intercepts of lines fitted to the phase 3 inflection in force recovery (Ford et al., 1977) extrapolated to the time of the midpoint of the step. To the extent that bridge detachment occurs at a uniform rate after the onset of the step and contributes to the slope of the records during phase 3, the T_2 intercept should reflect the average distance the attached bridges can move. This value, 14 nm, leads to our upper estimate of the ratio of intercepts. If, on the other hand, bridges detach at a more rapid rate before the time of the phase 3 inflection, the T_2 intercept overestimates the average distance a bridge can move. It seems unlikely, however, that the corrected intercept would be less than 9 nm, and this lower limit accounts for the lower limit of 2.5 in our estimate of the ratio of intercepts. This lower limit also agrees with the ratio of force to stiffness increase produced by the increased ADP.

The assumptions required to obtain this estimate should be kept in mind. These are 1) that the low-force bridges produce an average of zero force; 2) that the cross-bridges undergo a single power stroke per attachment cycle; 3) that the cross-bridge compliance does not vary among the different states; and 4) that all of the sarcomere compliance is in the cross-bridges, as suggested by Ford et al. (1981), but not by the more recent findings of others (Bagni et al., 1990; Huxley et al., 1994; Wakabayahsi et al., 1994; Higuchi et al., 1995).

Scaling and matching the records

The method of analysis used here assumes that the overall tension responses are the sum of the stochastic responses of

individual bridges. In this analysis, chemical interventions are assumed to alter only a fraction of the total population, leaving the remainder with normal responses. The responses of the altered bridges can therefore be estimated by subtracting the scaled reference record from the test response. Uncertainty in the method arises both because of uncertainty in the scale factor applied to the reference records and because only a fraction of the record can be matched. All of the methods suggest, however, that the detained bridges recover more slowly than the dominant parts of the transients. As expected of chemical transients, the rate constants for the recovery of detained bridges vary much less with step size than those responsible for most of the transients. The difference records in Figs. 7 and 9 also suggest that the recovery of these detained bridges could be delayed.

In the present experiments, suggesting detention of bridges in high-force states, it seems likely that most of the early, phase 2 responses could be attributed to nondetained bridges undergoing force-altering transitions. Thus the reference records were scaled to match the earliest responses. Because it is likely that the detained bridges will later move past the inhibited transition in the cycle while other, initially nondetained bridges will become detained, only the earliest recovery phase of the transients was matched. If the detained bridges did not alter the population of bridges cycling normally, the match could have been obtained simply by superimposing the records, as was done in Fig. 7. This result is not expected, however, because it is likely that the detention of bridges will diminish the population of normal bridges. It is possible that the data obtained with ADP could be explained entirely by this mechanism, because the reference record could probably be scaled down by a few percent without greatly distorting the flatness of the difference record. Such a mechanism could not explain the data obtained with reduced ATP, however, because the scale factor was substantially greater than unity. To make this mechanism tenable, therefore, it is necessary to postulate a second mechanism that increased the population of bridges that contributed to isometric force and responded normally to the sarcomere length changes, at least in the short term.

Additional mechanism

The scheme in Fig. 11 *A* suggests that lower MgATP or added MgADP caused bridges to be detained in the bare actomyosin state (rigor bridge) or the actomyosin-ADP state (ADP bridge). These detained bridges are likely to impose a load on the sliding filaments. The finding that the changes in the force-velocity curves can be explained, at least in part, by a small internal load is thus in keeping with the proposed scheme. The differences in the changes in both the force/stiffness ratios and the force-velocity properties seen with the two interventions further suggest that this is not the only mechanism responsible.

All of these deviations from the expected results would be explained if the detained bridges increased the activation of normal bridges and if the rigor bridges were substantially more effective than the ADP bridge. Moss et al. (1985) have found that the addition of troponin C, even to freshly prepared fibers, results in a greater calcium-activated force, presumably because even the fresh fibers have lost some troponin C during preparation. This observation raises the possibility that our skinned fibers might have been less than maximally activated under reference conditions, so that activation could be increased above that produced by high levels of calcium. A possible mechanism for this increase could be the cooperativity of cross-bridge binding. Because this cooperative binding is increased both by lowering the MgATP (Bremel and Weber, 1972; Godt, 1974) and by adding MgADP (Lu et al., 1993; Thirlwell et al., 1994), it is likely that activation would be increased by both interventions studied. To match the present results it must be postulated, however, that the rigor bridges were substantially more effective in increasing activation than the high-force bridges with ADP bound. Because cooperative activation is reduced during shortening, the reduction in intrinsic velocity not due to an internal load, represented by the decreased β in the ATP experiment, would be explained by reduction of cooperative activation by shortening at intermediate loads. To the extent that maximum velocity is independent of activation (Podolin and Ford, 1986), the changes in maximum velocity must be explained by another mechanism, such as the detained bridges imposing a load on the nondetained bridges. The combined effect of these two mechanisms is discussed quantitatively in the Appendix.

It should also be mentioned that Thirlwell et al. (1994) have suggested that the ADP bridge more effectively increases cooperative activation than the rigor bridge, the opposite of the mechanism postulated here. At present, we have no explanation for the difference between their conclusion and ours, but we should make two important points. First, their experiments did not test directly the effects of varying levels of rigor bridges produced by varying levels of ATP, and their conclusion derives mainly from the finding that their results could be explained entirely by the ADP bridge increasing cooperativity. Equally important is the fact that our experiments do not prove that a cooperative mechanism exists; they are simply consistent with this known mechanism increasing activation.

Chemical versus mechanical transitions

We make a distinction, which some may regard as artificial, between "physical" and "chemical" transitions. In this construct, physical changes are associated with movements of the bridge, such as by attachment, detachment, or force-altering steps, whereas chemical transitions, such as ATP hydrolysis or binding and unbinding of reactants, may not be associated with bridge movements. The reason for making this distinction is that the rate constants for physical transitions are likely to be altered by filament sliding, whereas the rate constants for the chemical transitions may

not be altered by sliding. The finding that the rate constants of the extra components of the transients seen in the presence of added ADP or lowered ATP varied less with step size than the other components of the response is in keeping with these interventions altering chemical transitions. The finding that the rate constants varied somewhat with step size can be explained by these chemical transitions being flanked by physical transitions that are sensitive to filament sliding. A steep increase in the rate of cross-bridge detachment with filament sliding (Huxley, 1957), for example, might explain the increase in the speed of the extra component of the phase 2 response with large releases.

Intrafiber gradients for reactants

The concentration gradients suggested by the velocity differences measured in the presence and absence of the ATP regenerating system were more than twice the values expected from the following calculations. These expectations derive, in part, from the conclusion of Kushmerick and Podolsky (1969) that the diffusion coefficients for solutes inside skinned fibers are about half the coefficients for the same constituents free in solution. The calculations suggest that the diffusion coefficients are reduced by about sixfold.

The concentration, C, at radius r of a substance that is consumed (or produced) by a reaction of rate R in a cylinder of radius r_o is related to its diffusion coefficient, D, by

$$C = C_o + R \cdot (r_o^2 - r^2)/4D \qquad (10)$$

when the external solution is stirred to maintain the concentration at the surface, C_o (Crank, 1957). Integrating this parabolic relationship over the radius of the cylinder indicates that the average concentration, C_a, of the substance within the cylinder is defined by

$$C_a = C_o + R \cdot r_o^2/8D \qquad (11)$$

The time-averaged reaction rate, R, under reference conditions was estimated to be 0.25 mM/s from the maximum power output of the fibers, ~13.5 mW/g. This value assumes a chemomechanical efficiency of 0.5, 55 kJ free energy/mol ATP, and an ATPase rate that averaged one-half the maximum value over the cycles of releases and restretches used here. If this last value were less, i.e., if the ATPase rate were less than half the maximum value, the calculated decrease in the diffusion coefficients would have to be greater than sixfold.

The fiber radii averaged ~27 μm. The radial diffusion coefficients within the fibers were expected to be half the published values for the same or similar size compounds in free solution (Kushmerick and Podolsky, 1969), leading to diffusion coefficients of 10^{-6} cm$^2 \cdot$ s^{-1} for MgATP and MgADP. Substituting these approximate values into Eq. 11 suggests a mean intrafiber MgADP concentration of 0.23 mM, 3 times less than the 0.7 mM suggested by the control experiments. This disparity led to the many control experiments described above, none of which could explain the large difference. Our inability to explain this difference suggests that the diffusion coefficients taken from the work of Kushmerick and Podolsky (1969) were too high, and leads to the following possible explanation of how the coefficients might be lowered in our preparation.

Diffusion of a solute in a matrix can be lowered by one of two mechanisms, binding and "tortuosity," the latter term denoting physical impediments to movement, such as tortuous channels or small pores in series with larger reservoirs. Because the solute is fixed when it is bound and free to diffuse normally when it is not bound, the diffusion coefficient will be lowered in proportion to the fraction of solute bound. In experiments such as these, in which the solute concentration greatly exceeds the concentration of binding sites, most of the solute will be free in solution. The effect of binding on diffusion rate is therefore likely to be small. To the extent that the effects of binding are small, the markedly lower diffusion coefficients suggest that there is substantially more tortuosity of the diffusion paths within our preparation compared both with free solution and with the skinned fiber experiments of Kushmerick and Podolsky (1969). At first sight this seems unlikely, because Kushmerick and Podolsky measured diffusion in skinned fibers. There is, however, a major difference in that the fiber lattice was compressed in the present experiments and not compressed in the experiments of Kushmerick and Podolsky. It seems likely that the tortuosity will be increased by the decrease in intrafilament distance. The present results would be explained if the sixfold reduction in radial diffusion coefficients were caused by greater tortuosity in the compressed lattice.

It should be mentioned that Cooke and Pate (1985) have calculated the intrafiber gradients in their preparation using diffusion coefficients more than 10 times less than those found by Kushmerick and Podolsky (taken from Mannherz, 1968, and Marston, 1973). The results presented here suggest that a value midway between the two previously determined values, approximately sixfold less than the diffusion coefficients in solution, would have been appropriate.

APPENDIX

The purpose of this appendix is to show that the results can be explained quantitatively if the two interventions, lowering ATP and raising ADP, produce two distinct populations of isometric bridges. One cycles normally, participates in the early parts of the transients, and is increased by the interventions creating the second population that is detained in high-force state(s) and contributes only a slow component to the transient force recovery. The following variables are considered:

N: Change in the fraction of attached, normally cycling bridges normalized to the number of bridges attached in the reference condition.

D: Fraction of bridges detained by the test intervention, normalized to the number of bridges attached in the reference condition.

F: Increase in isometric force in the test condition, normalized to the reference isometric force (0.25 for the ADP and 0.23 for the ATP experiments).

S: Increase in isometric stiffness in the test condition, normalized to the reference stiffness (0.10 for the ADP and 0.20 for the ATP experiments).

p: Ratio of average force generated by a detained bridge to the average force generated by an attached, normally cycling bridge. p is assumed here to be the same for the ADP and ATP experiments.

For the present calculations it is assumed that all sarcomere compliance is in the cross-bridges, as originally suggested by Ford et al. (1981), so that changes in stiffness reflect changes in cross-bridge number. If some sarcomere compliance is in the thin filaments, as suggested by more recent experiments (Bagni et al., 1990; Huxley et al., 1994; Wakabayashi et al., 1994; Higuchi et al., 1995), changes in sarcomere stiffness will still reflect changes in the number of attached cross-bridges, but stiffness measurements will underestimate these changes.

The observation that stiffness was increased significantly by these interventions indicates that the fraction of bridges attached in the reference condition was substantially less than 1. If it were not, there could be no increase in the fraction of attached bridges and therefore no stiffness increase. The detention of bridges would simply cause a shift of low-force attached bridges into high-force positions.

An estimate of the increase in the fraction of normally attached bridges can be gained from the following relationships:

$$F = N + p \cdot D \tag{A1}$$

$$S = N + D \tag{A2}$$

These equations cannot be solved exactly because of uncertainties in the values of p. Two solutions representing likely extremes are therefore presented.

For the first solution, the value of p is taken to be 2.5. This value derives from the consideration that if all of the 10% stiffness increase in the ADP experiment were due to detained bridges, the ratio of the force increase to the stiffness increase would be 2.5. If p had the same value in the ATP experiment, then 5% of the total of 23% force increase would be explained by 2% of the bridges being detained, whereas the remaining 18% of the force increase would be explained by an increase in normally cycling bridges. In this case, the ratio of detained bridges to force increase is ~0.09 in the ATP experiment and 0.40 in the ADP experiment. The ratio of these two ratios, 0.23 (0.09/0.4), is close to but not identical to the 0.33 ratio of internal loads calculated from the force-velocity data. An exact correspondence between the two would not be expected when isometric force is increased by cooperative activation, because shortening will reduce this cooperativity and cause activation to be lower at higher velocities.

The change in attached, normally cycling bridges can be estimated as the difference between the value found under the test condition minus the reference value corrected for the bridges detained. In the ADP experiment, for example, the suggestion that there was no change in the number of normally cycling bridges still implies an increase over the expected value; the detention of bridges is expected to reduce the pool available to cycle normally. The reduction in the pool depends on the fraction of bridges attached in the reference state. If this value is 0.5, the detention of bridges equivalent to 10% of the fraction normally attached would imply a 5% reduction in the pool. In the absence of a mechanism to increase normally cycling bridges, the number of normally cycling bridges should have been reduced by 5%. In this example, therefore, increasing ADP increased the attached, normally cycling bridges by 5%, whereas it increased the detained bridges by 10%. In the ATP experiment, the 2% detained bridges would be expected to decrease the normally cycling bridges by 1%. The finding of an 18% increase therefore implies a 19% increase in the normally cycling bridges associated with 2% detained bridges.

For the second solution, the value of p is taken to be 4, the ratio of the T_2 and T_1, as explained in the Discussion. When this value is substituted in Eqs. A1 and A2, the values for N and D become 0.05 and 0.05, respectively, in the ADP experiment and 0.19 and 0.01 in the ATP experiment. Again, the increase in normally cycling bridges is much greater and the addition of detained bridges much less in the ATP experiment.

The main conclusion of this appendix is that the increased force produced by the two interventions requires two mechanisms, one that detains bridges in high-force states and one that increases the fraction of bridges that are attached and respond normally. If the increase in the normally responding bridges is produced by the detained bridges, as through a cooperative effect on activation, then the rigor bridge is at least 10 times more effective in eliciting this mechanism than the ADP bridge.

Supported in part by U.S. Public Health Service grant RO1HL52760, a Senior Research Fellowship of the American Heart Association of Metropolitan Chicago to CYS, and grants from the Council for Tobacco Research and the American Heart Association of Metropolitan Chicago.

REFERENCES

Abbott, R. H., and G. H. Mannherz. 1970. Activation by ADP and the correlation between tension and ATPase activity in insect fibrillar muscle. *Pflugers Arch.* 321:223–232.

Andrews, M. A. W., D. W. Maughan, T. M. Nosek, and R. E. Godt. 1991. Ion-specific and general ionic effects on contraction of skinned fast-twitch skeletal muscle from the rabbit. *J. Gen. Physiol.* 98:1105–1125.

Bagni, M. A., G. Cecchi, F. Colomo, and C. Poggesi. 1990. Tension and stiffness of frog muscle fibers at full filament overlap. *J. Muscle Res. Cell Motil.* 11:371–377.

Bagshaw, C. R., D. R. Trentham, R. G. Wolcott, and P. D. Boyer. 1975. Oxygen exchange in the gamma-phosphoryl group of protein-bound ATP during Mg^{2+}-dependent adenosine triphosphatase activity of myosin. *Proc. Natl. Acad. Sci. USA.* 72:2592–2596.

Bremel, R. D., and A. Weber. 1972. Cooperation within actin filament in vertebrate skeletal muscle. *Nature New Biol.* 238:97–101.

Brenner, B. 1983. Technique for stabilizing the striation pattern in maximally calcium-activated skinned rabbit psoas fibers. *Biophys. J.* 41: 99–102.

Chase, P. B., and M. J. Kushmerick. 1988. Effects of pH on contraction of rabbit fast and slow skeletal muscle fibers. *Biophys. J.* 53:935–946.

Chiu, Y.-L., J. Asayama, and L. E. Ford. 1982. A sensitive photoelectric force transducer with a resonant frequency of 6 kHz. *Am. J. Physiol.* 243:C299–C302.

Chiu, Y.-L., S. Karwash, and L. E. Ford. 1978. A piezoelectric force transducer for single muscle cells. *Am. J. Physiol.* 253:C143–C146.

Cooke, R., and W. Bialek. 1979. Contraction of glycerinated muscle fibers as a function of the ATP concentration. *Biophys. J.* 28:241–258.

Cooke, R., and E. Pate. 1985. The effects of ADP and phosphate on the contraction of muscle fibers. *Biophys. J.* 48:789–798.

Crank, J. 1957. The Mathematics of Diffusion. Oxford University Press, London.

Dantzig, J. A., M. G. Hibberd, D. R. Trentam, and Y. E. Goldman. 1991. Cross-bridge kinetics in the presence of MgADP investigated by photolysis of caged ATP in rabbit psoas muscle fibres. *J. Physiol. (Lond.).* 432:639–680.

Ferenczi, M. A., Y. E. Goldman, and R. M. Simmons. 1984. The dependence of force and shortening velocity on substrate concentration in skinned muscle fibers from *Rana temporaria*. *J. Physiol. (Lond.).* 350: 519–543.

Ford, L. E., A. F. Huxley, and R. M. Simmons. 1977. Tension responses to sudden length change in stimulated frog muscle fibres near slack length. *J. Physiol. (Lond.).* 269:441–515.

Ford, L. E., A. F. Huxley, and R. M. Simmons. 1981. The relation between stiffness and filament overlap in stimulated frog muscle fibres. *J. Physiol. (Lond.).* 311:219–249.

Ford, L. E., K. Nakagawa, J. Desper, and C. Y. Seow. 1991. Effect of osmotic compression on the force-velocity properties of glycerinated rabbit skeletal muscle cells. *J. Gen. Physiol.* 97:73–88.

Godt, R. E. 1974. Calcium-activated tension of skinned muscle fibers of the frog. Dependence on magnesium adenosine triphosphate concentration. *J. Gen. Physiol.* 63:722–739.

Godt, R. E., and Lindley. 1982. Influence of temperature upon contractile activation and isometric force production in mechanically skinned muscle fibers of the frog. *J. Gen. Physiol.* 80:279–293.

Godt, R. E., and D. W. Maughan. 1988. On the composition of the cytosol of relaxed skeletal muscle of the frog. *Am. J. Physiol.* 254:C591–C604.

Godt, R. E., and T. M. Nosek. 1989. Changes of intracellular milieu with fatigue or hypoxia depress contraction of skinned rabbit skeletal and cardiac muscle. *J. Physiol. (Lond.).* 412:155–180.

Goldman, Y. E. 1987. Measurement of sarcomere shortening in skinned fibers from frog muscle by white light diffraction. *Biophys. J.* 52:57–68.

Higuchi, H., T. Yanagida, and Y. E. Goldman. 1995. Compliance of thin filaments in skinned fibers of rabbit skeletal muscle. *Biophys. J.* 69: 1000–1010.

Hill, A. V. 1938. The heat of shortening and the dynamic constants of muscle. *Proc. R. Soc. Lond. Biol.* 126:136–195.

Hoar, P. E., C. W. Mahoney, and W. G. L. Kerrick. 1987. MgADP increases maximum tension and Ca^{++} sensitivity in skinned rabbit soleus fibers. *Pflugers Arch.* 410:30–36.

Huxley, A. F. 1957. Muscle structure and theories of contraction. *Prog. Biophys. Biophys. Chem.* 7:255–318.

Huxley, A. F. 1974. Review lecture: muscular contraction. *J. Physiol. (Lond.).* 243:1–43.

Huxley, A. F., 1980. Reflections on Muscle. Princeton University Press, Princeton, NJ.

Huxley, A. F., and R. M. Simmons. 1971. Proposed mechanism of force generation in striated muscle. *Nature.* 233:533–538.

Huxley, A. F., and R. M. Simmons. 1973. Mechanical transients and the origin of muscle force. 1972 *Cold Spring Harb. Symp. Quant. Biol.* 37:669–680.

Huxley, H. E., A. Stewart, H. Sosa, and T. Irving. 1994. X-ray diffraction measurements of the extensibility of actin and myosin filaments in contracting muscle. *Biophys. J.* 67:2411–2421.

Kawai, M., and H. R. Halvorson. 1989. Role of MgATP and MgADP in the crossbridge kinetics in chemically skinned rabbit psoas fibers. *Biophys. J.* 55:595–603.

Kurebayashi, N., and Y. Ogawa. 1991. Discrimination of Ca^{2+}-ATPase activity of the sarcoplasmic reticulum from actomyosin-type ATPase activity of myofibrils in skinned mammalian skeletal muscle fibers: distinct effects of cyclopiazonic acid on the two ATPase activities. *J. Muscle Res. Cell Motil.* 12:355–365.

Kushmerick, M. J., and R. J. Podolsky. 1969. Ionic mobility in muscle cells. *Science.* 166:1297–1298.

Lu, Z., R. L. Moss, and J. W. Walker. 1993. Tension transients initiated by photogeneration of MgADP in skinned skeletal muscle fibers. *J. Gen. Physiol.* 101:867–888.

Lymn, R. W., and E. W. Taylor. 1971. Mechanism of adenosine triphosphate hydrolysis by actomyosin. *Biochemistry.* 10:4617–4624.

Mannherz, H. G. 1968. ATP-spaltung und ATP-diffusion in oscillierenden extrahierten Muskolfasern. *Pflügers Arch.* 303:230–248.

Marston, S. B. 1973. The nucleotide complexes of myosin in glycerol extracted muscle fibers. *Biochim. Biophys. Acta.* 305:397–412.

Moss, R. L., G. G. Giulian, and M. L. Greaser. 1985. The effects of partial extraction of TnC upon the tension-pCa relationship in rabbit skinned skeletal muscle fibers. *J. Gen. Physiol.* 86:585–600.

Podolin, R. A., and L. E. Ford. 1986. Influence of partial activation on the force-velocity properties of frog skinned muscle fibers in millimolar magnesium ion. *J. Gen. Physiol.* 87:607–631.

Reedy, M. K., K. C. Holmes, and R. T. Tragear. 1965. Induced changes in orientation of the cross bridges of glycerinated insect flight muscle. *Nature.* 207:1276–1280.

Seow, C. Y., and L. E. Ford. 1991. Shortening velocity and power output of skinned muscle fibers from mammals having a 25,000-fold range of body mass. *J. Gen. Physiol.* 97:541–560.

Seow, C. Y., and L. E. Ford. 1992a. ADP detains muscle cross-bridges near the end of their force producing power stroke. *Biophys. J.* 61:A294.

Seow, C. Y., and L. E. Ford. 1992b. Contribution of damped passive recoil to the measured shortening velocity of skinned rabbit and sheep muscle fibers. *J. Muscle Res. Cell Motil.* 13:295–307.

Seow, C. Y., and L. E. Ford. 1993. High ionic strength and low pH detain activated skinned rabbit skeletal muscle crossbridges in a low force state. *J. Gen. Physiol.* 101:487–511.

Taylor, E. W. 1992. Mechanism and energetics of actomyosin ATPase. *In* The Heart and Cardiovascular System, 2nd Ed. H. A. Fozzard, et al., editor. Raven Press, New York. 1281–1293.

Thirlwell, H., J. E. T. Corrie, G. P. Reid, D. R. Trentham, and M. A. Ferenczi. 1994. Kinetics of relaxation from rigor of permeabilized fast-twitch skeletal fibers from the rabbit using a novel caged ATP and apyrase. *Biophys. J.* 67:2436–2447.

Wakabayashi, K., Y. Sugimoto, H. Tanaka, Y. Ueno, Y. Takezawa, and Y. Amemiya. 1994. X-ray diffraction evidence for the extensibility of actin and myosin filaments during muscle contraction. *Biophys. J.* 67: 2422–2435.

White, A., P. Handler, E. L. Smith, and D. Steton. 1959. Principles of Biochemistry. McGraw-Hill Book Co., New York.

White, H. D., and E. W. Taylor. 1976. Energetics and mechanism of actomyosin adenosine triphosphatase. *Biochemistry.* 15:5818–5826.